Aalto University

OPEN ACCESS

This is an electronic reprint of the original article.
This reprint may differ from the original in pagination and typographic detail.

Kim, Sang Jin; Körgesaar, Mihkel; Ahmadi, Nima; Taimuri, Ghalib; Kujala, Pentti; Hirdaris, Spyros

The influence of fluid structure interaction modelling on the dynamic response of ships subject to collision and grounding

Published in:
Marine Structures

DOI:
10.1016/j.marstruc.2020.102875

Published: 01/01/2021

Document Version
Publisher's PDF, also known as Version of record

Published under the following license:
CC BY

Please cite the original version:
Kim, S. J., Körgesaar, M., Ahmadi, N., Taimuri, G., Kujala, P., & Hirdaris, S. (2021). The influence of fluid structure interaction modelling on the dynamic response of ships subject to collision and grounding. *Marine Structures*, *75*, Article 102875. https://doi.org/10.1016/j.marstruc.2020.102875

This material is protected by copyright and other intellectual property rights, and duplication or sale of all or part of any of the repository collections is not permitted, except that material may be duplicated by you for your research use or educational purposes in electronic or print form. You must obtain permission for any other use. Electronic or print copies may not be offered, whether for sale or otherwise to anyone who is not an authorised user.

Marine Structures 75 (2021) 102875

Contents lists available at ScienceDirect

Marine Structures

journal homepage: http://www.elsevier.com/locate/marstruc

The influence of fluid structure interaction modelling on the dynamic response of ships subject to collision and grounding

Sang Jin Kim [a], Mihkel Kõrgersaar [a,b], Nima Ahmadi [b], Ghalib Taimuri [a], Pentti Kujala [a], Spyros Hirdaris [a,*]

[a] Maritime & Arctic Technology Group, Department of Mechanical Engineering, Aalto University, Espoo, Finland
[b] Estonian Maritime Academy, Tallinn University of Technology, Tallinn, Estonia

ARTICLE INFO

Keywords:
Ship safety
Grounding
Collision
Fluid-structure interactions
Dynamic response
Structural crashworthiness

ABSTRACT

Analysis of the dynamic response of ships in accident scenarios requires a realistic idealisation of environmental and operational conditions by multi-physics models. This paper presents a procedure that simulates the influence of strongly coupled FSI effects on the dynamic response of ships involved in typical collision and grounding events. Our method couples an explicit 6-DoF structural dynamic finite element scheme with a hydrodynamic method accounting for (a) 6-DoF potential flow hydrodynamic actions; (b) the influence of evasive ship speed in the way of contact and (c) the effects of hydrodynamic resistance based on a RANS CFD model. Multi-physics simulations for typical accident scenarios involving passenger ships confirm that suitable FSI modelling may be critical for either collision or grounding events primarily because of the influence of hydrodynamic restoring forces.

1. Introduction

Ships in operation are exposed to various accidents (e.g. collisions, groundings, fires, explosions, etc.) that in turn may lead to serious Health, Safety and Environment (HSE) damages. According to Ref. [8] records from 2011 to 2018, 23,073 ship casualties have been recorded. Cargo ships were the most frequent ship segment at risk (48.6%), followed by passenger ships (20.7%). Accidental events resulted in 230 ship losses, 665 very serious casualties and 7694 person injuries. As shown in Fig. 1, 54.4% of casualties related to navigational accidents such as collision (26.2%), contact (15.3%), and grounding/stranding (12.9%).

Whereas it is broadly accepted that accidents involving oil tankers may cause serious environmental pollution [16], all types of accidents may relate to human factors and impact upon human life. The latter is particularly topical for modern cruise ships and RoPax vessels. Fig. 2 shows two representative collision and grounding events of relevance: (a) the collision of a cargo ship with MV St. Thomas Aquinas on Aug. 16, 2013 that lead to 108 deaths and 29 missing personnel [4]; (b) the grounding of Costa Concordia passenger vessel on Jan. 13, 2012 that led to 32 deaths [26]. The more recent collision of two Carnival passenger ships [5] and the grounding accident of Seatruck Performance RoPax [24] add on a list of events demonstrating the importance of mitigating risks associated with accidental events and their holistic consequences on people, safety and the maritime environment.

To prevent and minimise accidental damage effects, it is essential to account for risks in design (e.g. by accident prevention) and operations (risk control options for preparedness against damages). The Safety of Life at Sea [37] IMO regulatory instrument accounts

* Corresponding author.
E-mail address: spyros.hirdaris@aalto.fi (S. Hirdaris).

https://doi.org/10.1016/j.marstruc.2020.102875
Received 20 March 2020; Received in revised form 14 August 2020; Accepted 8 October 2020
Available online 21 October 2020
0951-8339/© 2020 The Authors. Published by Elsevier Ltd. This is an open access article under the CC BY license (http://creativecommons.org/licenses/by/4.0/).

for such risks for passenger and cargo ships other than Bulk Carriers and Tankers originally stipulated in Refs. [15] Common Structural Rules (CRS). SOLAS regulations idealise the influence of collision and grounding events by box-like damage extents [6]. Notwithstanding, it may be useful to evaluate the influence of realistic operational and environmental conditions on damage; especially considering that [37] do not account for the influence of sea environmental on crashworthiness, and in turn possible effects of more realistic damage extents on ship stability under extreme events (e.g. conditions associated with serious flooding).

The literature presents various models and procedures on collision and grounding mechanics using experimental, numerical and analytical methods [34]. For example, for the case of collision [7], performed a large-scale test and developed a Finite Element Model (FEM) procedure on the collision resistance of an X-core structure [22]. developed a simplified method for the analysis of ship crashworthiness following a series of experimental and numerical investigations on ship bottom damages following grounding [27]. studied the effect of rock size and friction coefficients for a two-hold cargo section. More recently [32], studied the effects of rock-ship structure interactions for the case of deformable rocks. A critical review of various studies that focused on the derivation and validation of simplified models (e.g. [10, 11, 29, 30, 31, 36, 44-47] leads to the conclusion that from dynamic response perspective the approach of [36] could be perceived as the most practical. The effects of collision parameters on structural response characteristics have also been studied by other authors such as [14, 29-31] and [11]. However, all these models consider only part of the ship (e.g., 1–2 cargo holds, bottom/side structures, etc.) and apply restrictions in 6 Degree of Freedom (DoF) structural dynamics. They also neglect the combined seakeeping/manoeuvring influence of hydrodynamic effects on dynamic response. In an attempt to take into account some of these effects, [20,21] developed the subroutine MCOL in LS-DYNA and applied the method to evaluate the structural response following a ship-submarine collision event [43]. introduced a structural analysis procedure by coupling LS-DYNA with a potential flow seakeeping solver. More recently [33], carried out a Fluid-Structure Interaction (FSI) analysis by coupling an Arbitrary Lagrangian-Eulerian (ALE) method with FEM and compared results against MCOL. Their prediction is body exact (Level 4 method as per [12] and therefore accounts for the combined effects of fluid motions on FEM. However, it is computationally uneconomic and does not account for other multi-physics effects such as the combined influence of ship hydrodynamics, evasive velocity in the way of contact and ship resistance on dynamic response.

In this paper we introduce a 3D FSI model that combines the influence of 6-DoF seakeeping/manoeuvring and ship resistance with an explicit FEM scheme. Along these lines we present a novel and practical procedure that models the combined effects of ship dynamics in waves on ship crashworthiness and dynamic response (see section 2 and Table 1). Applied examples of relevance focus on passenger ships subject to typical collision and grounding events are presented (see section 3) with the aim to conclude the influence of realistic multi-physics assumptions on dynamic response (see section 5).

2. An FSI procedure for ship structural crashworthiness

Fig. 3 illustrates a novel multi-physics procedure for the analysis of the structural dynamic response and, consequently, structural crashworthiness of ships subject to collision and grounding events. The methodology comprises three parts, namely: (a) wet analysis in still water conditions; (b) dry structure modelling and (c) FSI modelling/analysis. The wet analysis module accounts for (i) the impact velocity in the way of contact following evasive action; (ii) the influence of surrounding water following potential flow radiation/diffraction hydrodynamics leading in turn to the estimation of restoring, added mass and wave damping forces, and (iii) the influence of hydrodynamic resistance in still water conditions. Dry modelling involves the development of a 3D FEM. This model idealises all longitudinal and transverse elements of the ships involved in a collision or grounding scenarios as well as the condition of sea bottom for a grounding scenario. The ships are modelled as deformable structures. However, the seabed rocks are idealised as rigid bodies. In the FSI modelling/analysis, boundary and loading conditions on an explicit FEM solver stem from hydrodynamic actions. Consequently, a coupled FSI scheme is employed to assess nonlinear dynamic response (reaction forces and moments) at each time step (see section 3). LS-DYNA [23] was used for FEM. Hydrodynamic actions following seakeeping analysis (e.g. added mass, restoring force, damping forces etc.) were evaluated with BV Hydrostar [1] solver. This enabled coupling the seakeeping actions with structural response in MCOL [9]. The impact velocity in the way of contact was evaluated independently using the method of [40]. For both grounding and collision simulations, resistance forces accounting for forward speed effects were evaluated using STAR CCM+ [38] and were directly applied to the FEM. The simulation assumed fixed terms of hydrodynamic properties in intact conditions. Table 1 summarises assumptions applied in past existing approaches and the method introduced in this paper. As shown in Table 1, this study considers a more realistic situation of ships in grounding and collision than existing approaches.

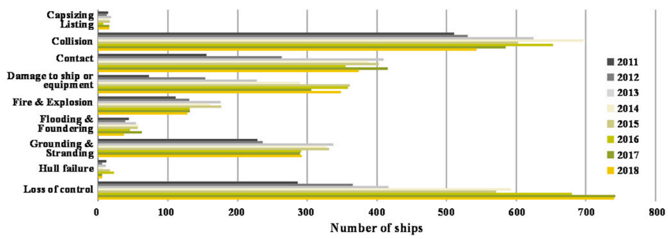

Fig. 1. Distribution of casualty events with a ship during 2011–2017 [8].

3. Study case

3.1. Target structures

Table 2 and Figs. 4 and 5 illustrate the two target ships, namely passenger ship (Ship A) and Ro-Pax ship (Ship B) used in this study. Ship A was used to model for both collision (struck by Ship B) and grounding simulations.

3.2. Accident scenarios

3.2.1. Collision scenario

For the collision scenario, the variables considered were: (a) speed, (b) displacement, (c) location and (d) angle. Review of the statistical analysis of collision accidents presented by Ref. [28] suggests that a realistic operational scenario leading to serious damage is reflected to striking/struck ship velocity ratio of the order of 2.5. This ratio corresponds to the upper 30% range of available ship samples and as such, was perceived as representative enough for this study. Fig. 6 demonstrates a collision event when striking ship B is progressing with speed of 5 knots along surge direction while struck Ship A progresses with surge speed of 2 knots at 90° to Ship B. Both ships were assumed to operate in fully loaded conditions with the collision event taking place in the way of the centre of the transverse bulkheads at amidships of ship A.

3.2.2. Grounding scenario

For the grounding scenario, the variables considered were: (a) speed, (b) location and (c) rock geometric properties [37]. provides bottom damage characteristics for passenger and cargo ships other than oil tankers as presented in Table 3. Based on these regulations, the maximum damage extents of Ship A were evaluated as 12.8 × 5.37 × 1.61 (m) in longitudinal, transverse and vertical directions respectively. The rock was modelled as rigid with dimensions shown in Fig. 7(a). It is noted that the rock height accounted for the double bottom height (= 1.6 m) of Ship A, and grounding was assumed to progress along the centerline of the vessel. Such a scenario could possibly lead to a serious flooding event. The ship has 11 knots of grounding speed in way of contact. This corresponds to the mean grounding speed of passenger ships (including RoPax) [42].

3.3. The influence of operations and environmental conditions

3.3.1. Impact velocity in 6-DoF

A manoeuvring analysis tool that calculates the velocity in 6-DoF following an evasive manoeuvre has been developed by Ref. [39] based on Matusiak's model [25]. The model used a 4th order Runge-Kutta numerical integration to account for the ship equations of motion at each time step by the following 6 × 6 system of matrix equations:

$$[M+M_a]\left\{\ddot{X}\right\}+[F_D]\left\{\dot{X}\right\}+[F_R]\{X\}=[F_{C1}]+[F_{C2}]+[F_E] \tag{1}$$

where $[M]$ and $[M_a]$ are the structural mass/inertia and added mass/inertia matrices, $\{\ddot{X}\}$, $\{\dot{X}\}$ and $\{X\}$ are the acceleration, velocity and displacement, $[F_D]$ is the damping force, $[F_R]$ is the restoring force, $[F_{C1}]$ is the Coriolis and centripetal forces, $[F_{C2}]$ is the control force including resistance, propeller and rudder forces, and $[F_E]$ is the environmental force by wind and waves, respectively.

The manoeuvring simulation was carried out in calm water conditions and at a low speed of ship; thus, out of plane motions were assumed to be almost zero before the impact according to the model presented by [39,40]. Consequently, the impact velocity in the way of contact for collision and grounding simulations have been obtained and applied to the FE model (see Table 4) for both collision and grounding scenarios described in section 3.2.

3.3.2. Hydrodynamic properties

As per [20]; MCOL was used to solve seakeeping in 6-DoF:

(a) MV St. Thomas Aquinas collision disaster (striking ship)

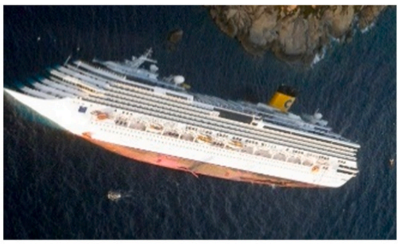

(b) Costa Concordia grounding disaster

Fig. 2. Examples of (a) collision and (b) grounding accidents.

Table 1
Comparison of assumptions between existing approaches and the new method.

References	Method				Extent of target structures	Hydrodynamic properties	Impact velocity	Resistance force
	T	A	FEM	FSI				
[14]	x	x	x		Plated girder	–	Surge	–
[7]	x		x		Partial structure	–	Surge	–
[27]			x		2 cargo holds	Partially	Surge and heave	–
[11]		x	x		X-core structure	–	Surge	–
[44]		x	x		A cargo hold	–	Surge	–
[22]	x	x	x		Partial stiffened panel	–	Surge	–
[43]			x		Partial structure	All properties	Surge	–
[45]	x	x	x		Plate for test and analytical/a cargo hold for FEM	–	Surge	–
[32]			x		Partial of bottom	–	Surge	–
[47]		x			Entire ship	Added mass	Surge	–
[33]			x	x (ALE)	Entire hull and partial structure	All properties	Surge	Yes (ALE)
Present study			x	x (MCOL)	Entire ship	All properties	6 DoF	Yes (RANS CFD[a])

[a] Note: T: laboratory test (experiment), A: Analytical method, FEM: Finite Element Method, FSI: Fluid Structure Interaction method, ALE: Arbitary Langragean Eulerean FSI scheme, MCOL: LS-DYNA subroutine program, RANS CFD: Reynolds Averaged Navier Stokes Computational Fluid Dynamics solver.

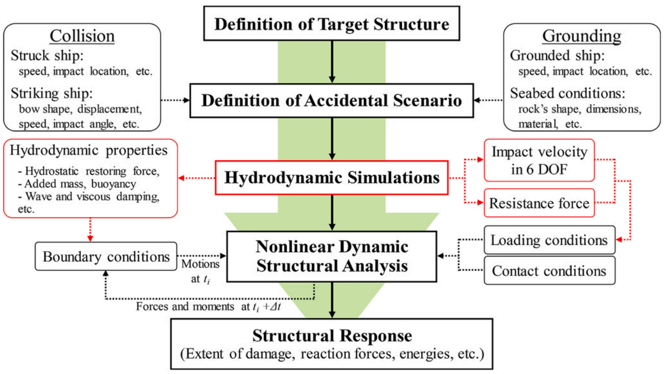

Fig. 3. Procedure for dynamic response analysis of ships subject to collisions and groundings.

Table 2
Principal dimensions of target ships.

	Ship A	Ship B
Length overall (m)	238.0	221.5
Breadth (m)	32.2	30.0
Design draught (m)	7.2	6.9
Gross tonnage (tonnes)	63,000	45,000
Block coefficient	0.661	0.578

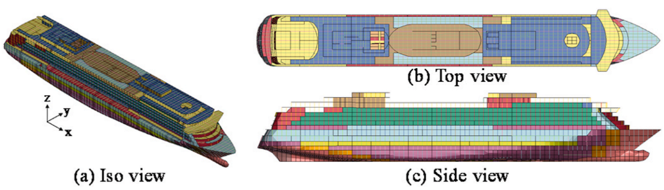

Fig. 4. Passenger ship (Ship A) for both collision (struck) and grounding.

$$[M + M_a][\ddot{x}] + [G][\dot{x}] = [F_R(x)] + [F_D(x)] + [F_V(x)] + [F_C] \tag{2}$$

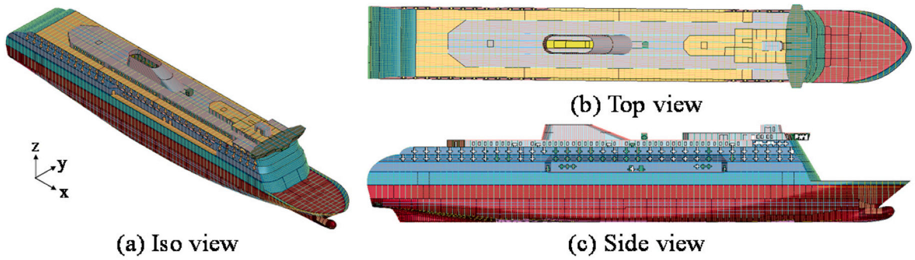

Fig. 5. Ro-Ro passenger ship (Ship B) for collision (striking).

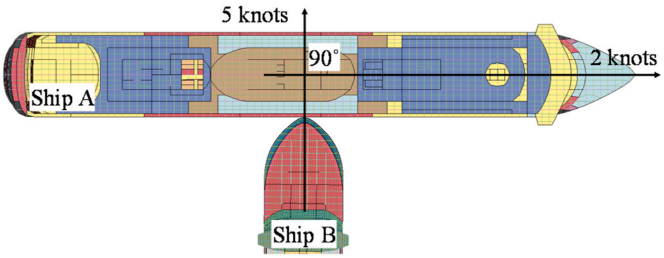

Fig. 6. Collision scenario.

Table 3
Bottom damage characteristics for passenger ships [37] (L: ship length; B: ship breadth).

Longitudinal extent (m)	$min.\{(L^{2/3})/3, 14.5\}$	
Transverse extent (m)	$min.\{B/6, 10\}$ For 0.3L from the F.P. of the ship	$min.\{B/6, 5\}$ Any other part of the ship
Vertical extent from the keel line (m)	$min.\{B/20, 2\}$	

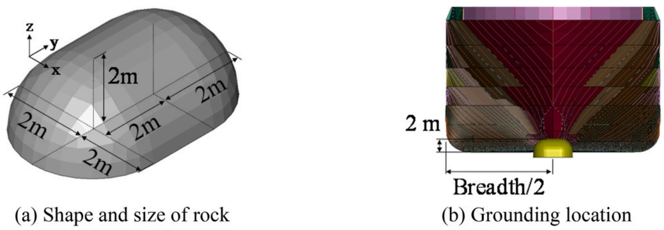

Fig. 7. Definition of rock and impact location.

Table 4
Initial impact velocity for collision and grounding obtained by the maneuvering analysis.

Events	Ship	Surge (m/s)	Sway (m/s)	Heave (m/s)	Roll (°/s)	Pitch (°/s)	Yaw (°/s)
Collision	A	1.0280	0.1510	0.0000	0.0000	0.0000	−0.0770
	B	2.5700	0.4510	−0.0007	0.0000	−0.0003	−0.1920
Grounding	A	5.6590	−0.1470	−0.0009	−0.0240	−0.0021	0.3070

where x is the earth-fixed Centre of Gravity (CoG) of the ship, $[M]$ and $[M_a]$ are the structural mass/inertia and added mass/inertia matrices, $[G]$ is the skew-symmetrical gyroscopic matrix, and $[F_R]$, $[F_D]$, $[F_V]$ and $[F_C]$ are the hydrostatic restoring, wave damping, viscous and contact forces, respectively. It is noted that the left-hand side terms of Eq. (2) are body fixed terms and the right-hand terms depend on the ship's motion.

The generalised structural mass (M) and the added mass matrices (M_a) in 6-DoF were defined as:

$$M = \begin{bmatrix} m & 0 & 0 & 0 & 0 & 0 \\ 0 & m & 0 & 0 & 0 & 0 \\ 0 & 0 & m & 0 & 0 & 0 \\ 0 & 0 & 0 & I_{xx} & -I_{xy} & -I_{xz} \\ 0 & 0 & 0 & -I_{xy} & I_{yy} & -I_{yz} \\ 0 & 0 & 0 & -I_{xz} & -I_{yz} & I_{zz} \end{bmatrix} \tag{3}$$

$$M_a = \begin{bmatrix} m_{11} & 0 & m_{13} & 0 & m_{15} & 0 \\ 0 & m_{22} & 0 & m_{24} & 0 & m_{26} \\ m_{31} & 0 & m_{33} & 0 & m_{35} & 0 \\ 0 & m_{42} & 0 & m_{44} & 0 & m_{46} \\ m_{51} & 0 & m_{53} & 0 & m_{55} & 0 \\ 0 & m_{62} & 0 & m_{64} & 0 & m_{66} \end{bmatrix} \tag{4}$$

where m is the mass of ship, I_{xx}, I_{yy} and I_{zz} are the mass moments of inertia in each direction, I_{xy}, I_{yz} and I_{xz} are the bi-products of inertia, respectively in way of the three dimensional reference system; m_{ij} is an added mass in the ith-direction caused by an acceleration in jth-direction assuming port/starboard symmetry [35].

The restoring force related with the water plane area (see term $[F_R]$ in Eqs. (1) and (2)), was expressed by the hydrostatic restoring matrix (K) as:

$$K = \rho g \begin{bmatrix} 0 & 0 & 0 & 0 & 0 & 0 \\ 0 & 0 & 0 & 0 & 0 & 0 \\ 0 & 0 & A_W & A_W \cdot y_W & -A_W \cdot x_W & 0 \\ 0 & 0 & A_W \cdot y_W & J_{Wx} & -J_{Wxy} & 0 \\ 0 & 0 & -A_W \cdot x_W & -J_{Wxy} & J_{Wy} & 0 \\ 0 & 0 & 0 & 0 & 0 & 0 \end{bmatrix} \tag{5}$$

where ρ is the density of water, g is the gravitational acceleration, A_W is the area of waterplane, x_W and y_W are the centre of area in each direction, J_{Wx} and J_{Wy} are the second moment of inertia of waterplane area, and J_{Wxy} is the product of inertia, respectively.

In MCOL, frequency-dependent wave damping matrices represent the influence of wave memory effects. In the idealisation presented 0.1–2.5 rad/s of frequencies with 0.1 interval were applied to account for wave damping forces. The relationship between viscous force and moments may change depending on the ship's speed. However, forward speed parameters were assumed zero on the

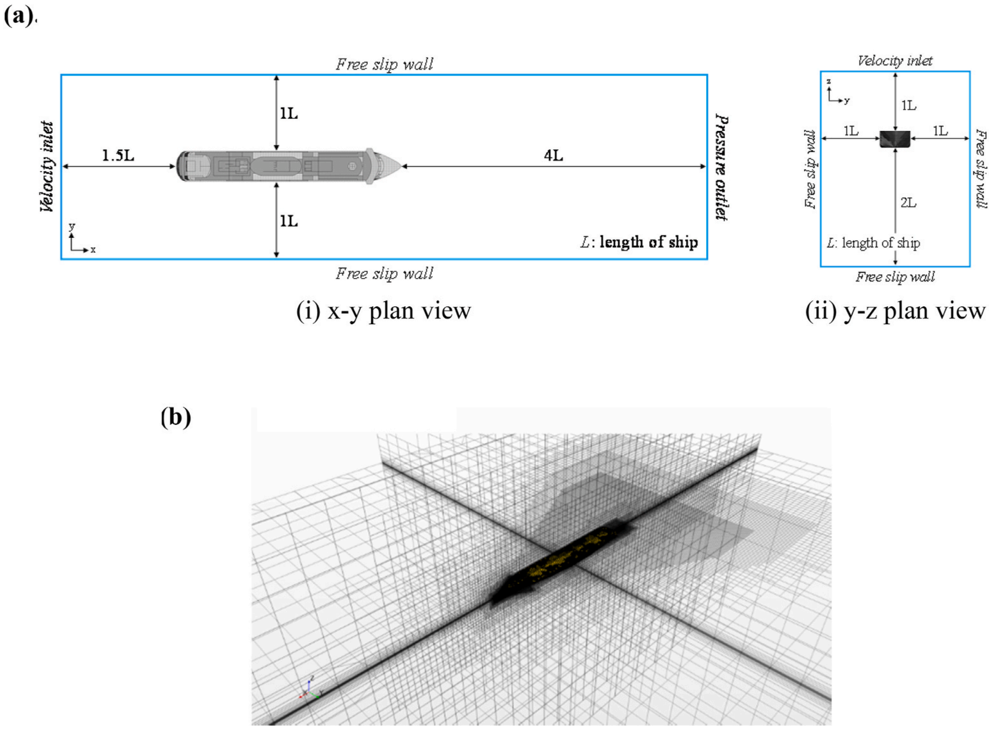

Fig. 8. (a)Computational domain and boundary conditions in STAR CCM+.(b)Generated grids (3D view) us/ed in CFD simulations of STAR CCM+ (Total number of grids = 4.3 million (0.6 million for coarse, 1.2 million for medium and 2.5 million for fine mesh) in this CFD simulation.

basis that: (i) speeds for the case of either collision or grounding events were low, and the wave environment was considered calm; (ii) in hydrodynamic terms the relationship between ship's speed and viscous damping is prone to various uncertainties [3,12].

3.3.3. Resistance force

In traditional naval architecture the resistance force is generally related to ship speed as per [13]. For the purpose of this investigation it was assumed that during the collision scenario the struck ship experiences a primary resistance force in beam seas because of sway motions on her side shell. The influence of resistance force on surge dynamics of the striking ship during the collision event and for the case of the grounding scenario were idealised by the STAR CCM+ (2019) Reynolds-Averaged-Navier-Stokes (RANS) solver. A $k-\varepsilon$ turbulence model and the Finite Volume Method (FVM) were used for the evaluation of velocity-dependent resistance forces [2]. The Volume of Fluid (VOF) method was used to idealise the water-air interaction in the way of the water free surface. Fig. 8(a) shows the computational domain and boundary conditions used in these simulations. The automated mesh option in STAR-CCM+ was used to generate the trimmed hexahedral mesh with additional refinement at some critical part of the domain such as the zone near to the hull, free surface and leading edge of the plates. For best accuracy, the thickness of the first prism layer was defined such that the $y+$ magnitudes are always greater than 30. A fine mesh scheme was used and the grid computational domain is shown in Fig. 8(b).

Calculated resistance forces for ships with forward (surge) speeds for the striking/grounded ships and sway speed for the struck ship are shown in Fig. 9. Fig. 10 shows the ship speed during the accident and resistance force-time histories that were applied in the way of the centre of gravity of the finite element model.

4. Finite element (FE) modelling

The LS-DYNA [23] explicit nonlinear FE solver was used to analyse the dynamic response for both collision and grounding scenarios. The FE model comprises of shell elements idealising the 2-dimensional structure (plate) and beam elements for modelling the 1-dimensional members (stiffeners, beams, columns, etc.). Shell elements use the Belytschko-Tsay formulation that accounts for the translational and rotational velocity of nodes in 6 DoF [23]. Beams are modelled according to the Hughes-Liu with cross-section integration model that allows for the implementation of user defined cross sections [23].

The influences of operations and environmental conditions were applied as per section 3.3. FEM assumed that both ships are made of mild steel (see Table 5). This may be considered adequate as in passenger ships only few structures are made of aluminium or anisotropic material. The structural dynamic effects of strain rate depend on impact velocity and were implemented by the Cowper-Symonds equation (see Eq. (6)) [18]:

$$\sigma_{Yd} = \left[1 + \left(\frac{\dot{\varepsilon}}{C}\right)^{1/q}\right]\sigma_Y \tag{6}$$

where σ_{Yd} and σ_Y are the yield strength in static and dynamic loads, $\dot{\varepsilon}$ is the strain rate, and C and q are material related coefficients (Cowper-Symonds coefficients).

To suitably idealise fracture criteria, a dynamic fracture strain factor of the order of 0.1 was considered. The strain factor is by definition velocity-dependent and accordingly varies depending on the strain rate. However, based on the work of [17,19] the constant value of 0.1 that may be considered representative enough especially for ships subject to collision or grounding events was used in this study. To idealise the ship – ship contact during collision and ship-rock contact during grounding the so-called '*surface to surface contact option*' and '*single surface contact option*' of LS-DYNA were applied. The latter accounts for self-contact in fractured or folded structures [23]. The static and dynamic friction coefficient used in these contact options was 0.3 [19]. Table 6 summarises results from a mesh convergence study that focused on displacements obtained on the port side of the struck vessel during collision. As expected, initial

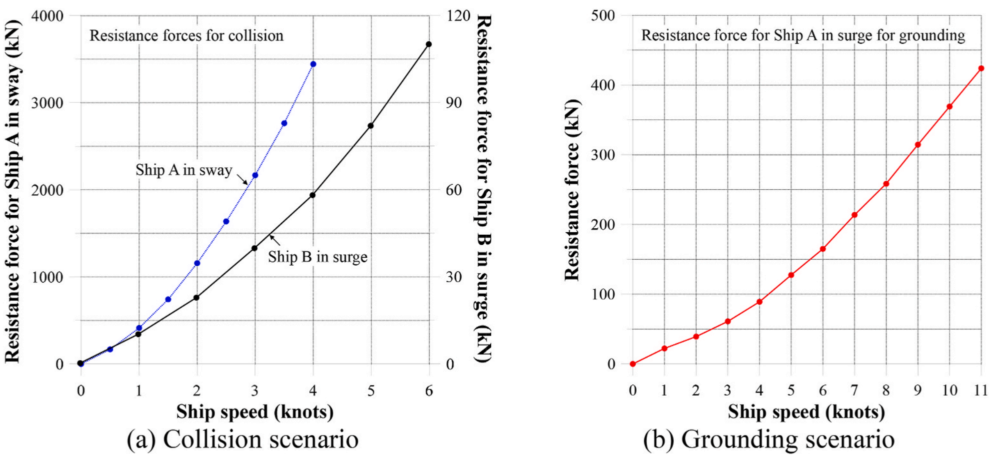

Fig. 9. Resistance force vs. speed for collision and grounding scenarios.

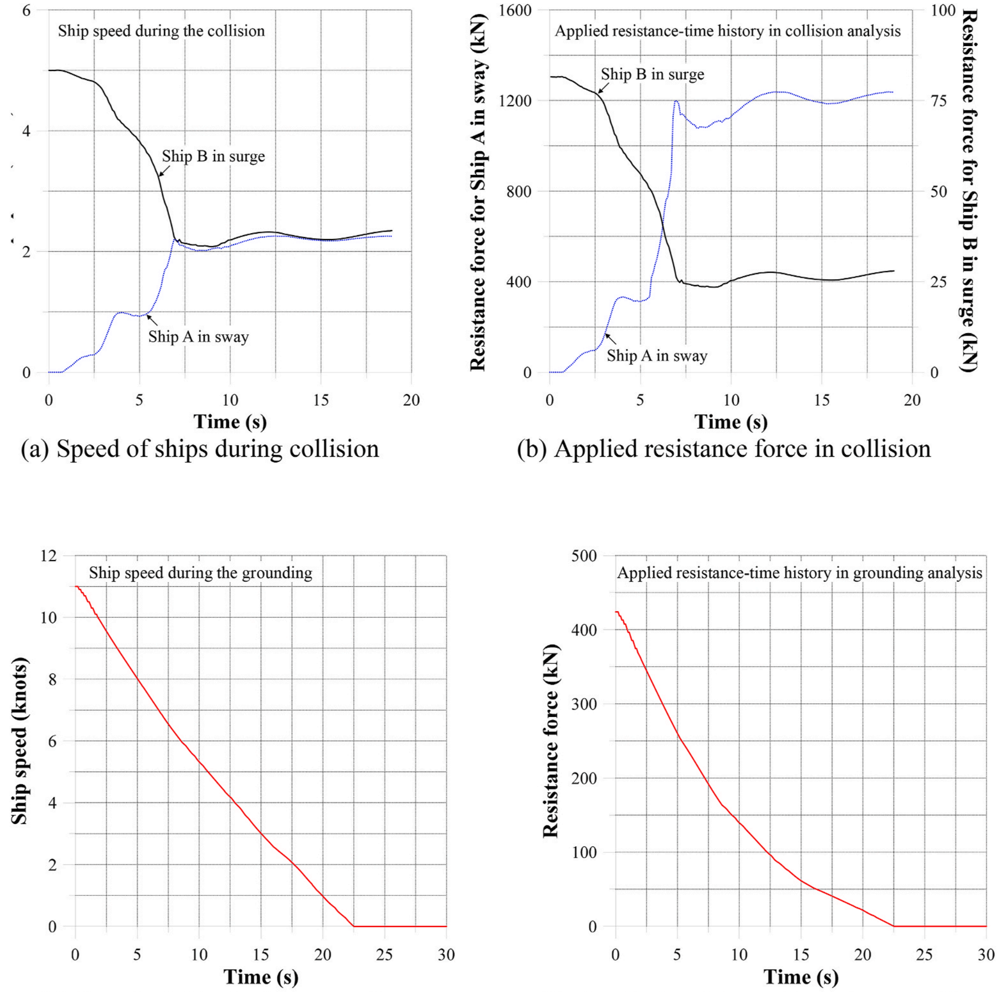

(a) Speed of ships during collision (b) Applied resistance force in collision

(c) Speed of ship during grounding (d) Applied resistance force in grounding

Fig. 10. Applied resistance force-time history for collision and grounding scenarios.

Table 5
Material properties applied in the present study.

Density (kg/m^3)	Yield strength (MPa)	Young's modulus (GPa)	Cowper-Symonds coefficients		Dynamic fracture strain (–)
			C	*q*	
7850	235	205.8	40.4	5	0.1

Table 6
Results of mesh convergence study.

Ref. element size (mm)	Maximum response		Difference*	
	Penetration (m)	Absorbed energy (MJ)	Penetration	Absorbed energy
150	13.12	78.64	1.00	1.00
200	13.40	79.14	1.02	1.01
250	14.36	80.57	1.09	1.02
300	14.49	82.66	1.10	1.05

Note: * is the ratio between results by using 150 mm element and each element size.

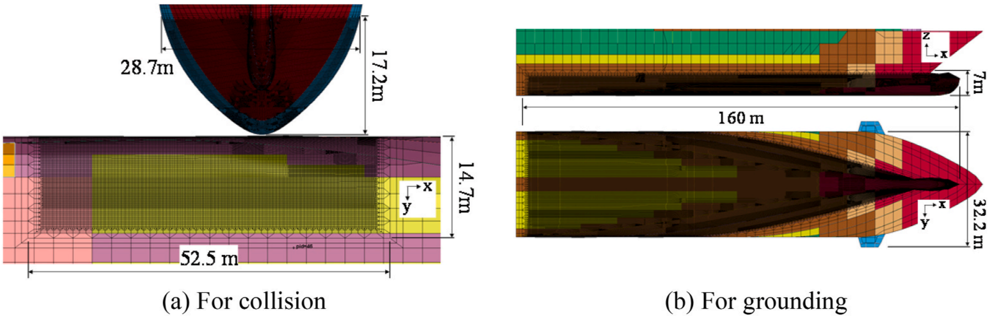

Fig. 11. FE models with refined element zone for FE simulations.

penetration was observed at the tip of the striking ship's bow where the first contact took place. Based on engineering experience [19, 41], the optimum element edge size of 200 mm was selected and applied in the way of the expected damage area (see Fig. 11).

To idealise the influence of multi-physics (i) hydrostatic and seakeeping properties; (ii) the evasive speed in the way of contact and (iii) hydrodynamic resistance were applied as boundary conditions. The combined effects of all these simulations were run on a supercomputing facility using 6 cores of CPU and 12 GB of RAM over 10 days and simulations assumed durations of 40 s for the collision event and 60 s for the grounding event.

The collision analysis modelling technique was validated with the analytical approach introduced by Liu et al. [48]. Accordingly, the internal energy (E) comprising of the absorbed and frictional energy of the striking ship with 90 deg. of collision angle (Eq. (7)) is given as:

$$E = \frac{1}{2}\frac{1}{D_x - \frac{k_x}{k_y}D_y}V_{ax}^2 \tag{7}$$

where D_x, D_y, k_x and k_y represent respectively factors regarding the mass/added mass, breadth, collision location of striking and struck ships, and V_{ax} is the velocity of striking ship Liu et al. (2017).

The analytical method gives 60.385 MJ of internal energy. The internal energy by the numerical analysis with hydrodynamic properties was 59.03 MJ (of which 32.93 MJ corresponded to absorbed energy and 26.10 MJ to the frictional energy). This confirmes that the modelling technique adopted in this study is reasonable. Based on the adequacy of the collision simulations, the same modelling technique was implemented for the grounding FE analysis.

5. Dynamic response

5.1. The influence of velocity in way of contact

Figs. 12 and 13 demonstrate comparisons of structural dynamic responses (penetration, grounding length and absorbed energy) for both collision and grounding scenarios. Simulations accounted for the influence of surge velocity in way of contact following 6-DoF

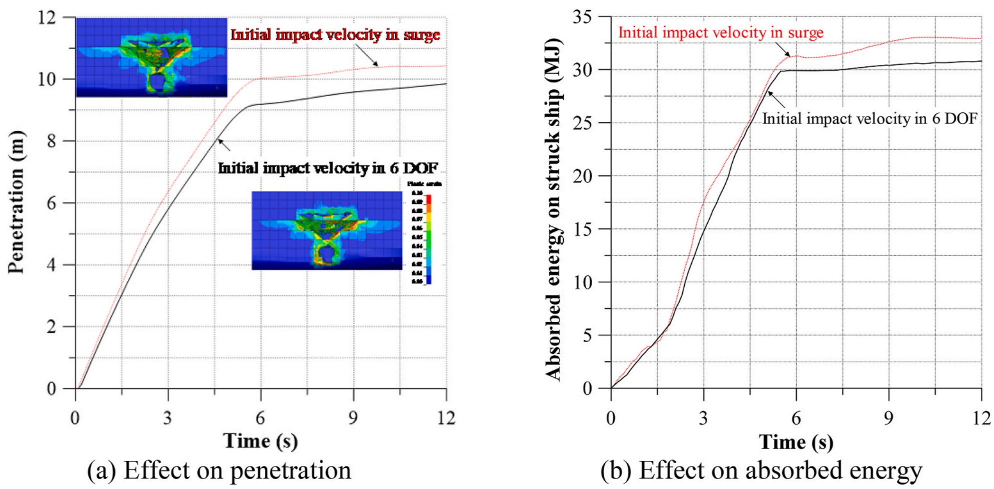

Fig. 12. Effect of initial impact velocity in collisions.

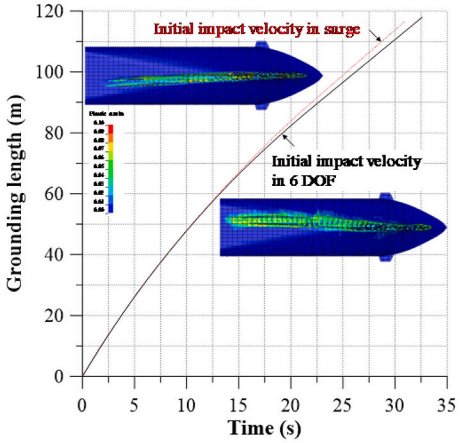

(a) Effect on grounding length

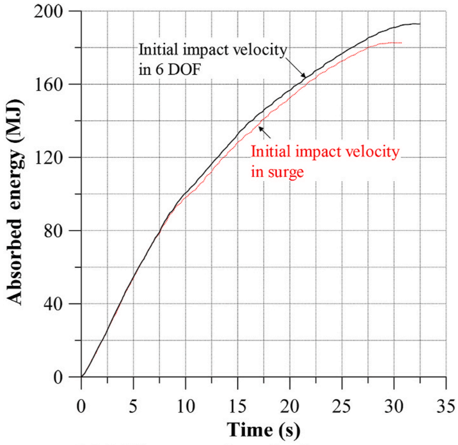

(b) Effect on absorbed energy

Fig. 13. Effect of initial impact velocity in groundings.

maneuvering analysis as per [40]. For the collision scenario, initial impact velocities in the sway motion of the struck ship and the surge motion of striking ship (following zig-zag maneuvering analysis) are shown in Table 4. Results demonstrate an 8% maximum difference in the dynamic response with and without accounting for the influence of impact velocity (i.e. maneuvering effects) (see Fig. 12(a)). For the case considered this could be attributed to the decrease in the relative speed between struck and striking ships in way of contact. On the other hand, for the grounding scenario the influence of maneuvering on the grounding length was minor. This is because the ship forward speed of 11 knots of surge motion dominated the magnitude of the damage length. However, the absorbed energy of the grounded ship seemed to be influenced more by the combined sway and roll motions on impact speed. In conclusion, it appears that ship damage extents pertaining to either collision or grounding events may be influenced by the magnitude of surge motions associated with forward speed. In addition:

- For collision, the impact velocity may directly affect the horizontal and vertical extents of damage. However, pitch motion of the striking ship could further amplify the energy and thus increase further these damage extents. In addition, the sway velocity of struck ship affects structural reponses due to the relative velocity. For example, the sway velocity of the struck ship which has the same direction with the surge velocity of the striking ship may lead to smaller damage than the one the ship would experience in an opposite to the striking ship (see Figs. 12 and 13).
- For grounding, heave, pitch and roll motions seem to affect ship damage extents.

5.2. The influence of surrounding water

Fig. 14 shows how different hydrodynamic actions (e.g. added mass, damping, restoring forces) may affect ship response. When all hydrodynamic properties are considered the energy influencing the dynamics of the struck ship becomes higher. Thus, the extents of damage may increase (see Fig. 14(d)) as compared to more simplified simulation cases (e.g. without added mass, restoring force, etc.). When damping matrices are considered, the energy appears to be a marginally lower due to the different energy dissipation mechanism. On the other hand, added mass effects seem to marginally influence the energy absorbed by the structure in comparison to restoring forces. Instead they seem to have greater significance upon the absorbed energy and penetration margins imposed upon the struck and striking ships (see Fig. 14(d) and (f)). Fig. 15 demonstrates representative extents of damage on the struck ship 12 s after the first contact. This time window is considered satisfactory in terms of obtaining converged results and therefore the idealisations represented may be considered realistic. Hydrodynamic damping effects progressively reduce as motion effects decay following collision (Fig. 14(c)). Fig. 16 presents the sway and roll motions of the struck ship. It also shows that the restoring forces affect sway and roll motions, and the added mass on struck ship predominantly influences the sway motion of the ship.

Fig. 17 demonstrates results from grounding analysis. The maximum extent of damage along the length direction when added mass effects are not accounted for is longer by 10.3% in comparison to results accounting for added mass. The influence of the restoring force on grounding length is even more significant. This is possibly because of the grounded ship sharp rotations in pitch direction after her first contact with the rigid rock. The mechanism of grounding and collision are similar. In both cases the influence of hydrodynamic damping forces in the response reduce the absorbed energy by structures (Figs. 17(c) and Fig. 14(c)). Fig. 18 illustrates the extents of damage at the end of the grounding event when reaction forces are negligible. A few seconds after the initial impact, there are small damages in way of the bow as there is no restoring force and the grounded ship tends to rapidly ride up and rotate (see Figs. 17(b) and 18(d)).

Hydrodynamic actions affect grounded and struck ships in different ways. For example, the added mass of the object in groundings influences the kinetic energy dissipation (see Fig. 18(a) and (b)). On the other hand, added mass effects on the struck ship may lead to increase in the ship's total weight (self-weight + added mass) and therefore makes the struck ship's sway movement slower (1.058/

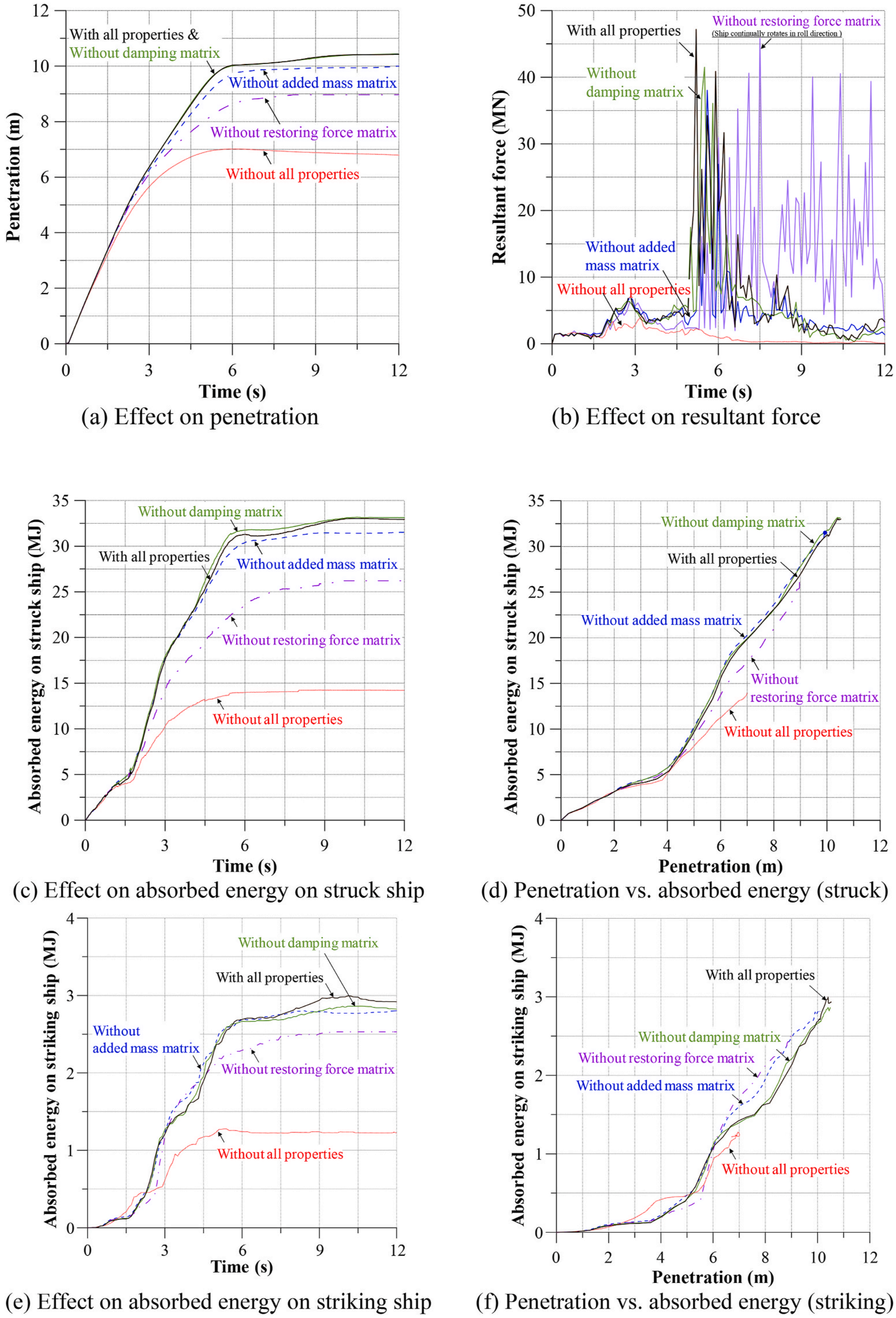

Fig. 14. The influence of hydrodynamic properties in collision scenario.

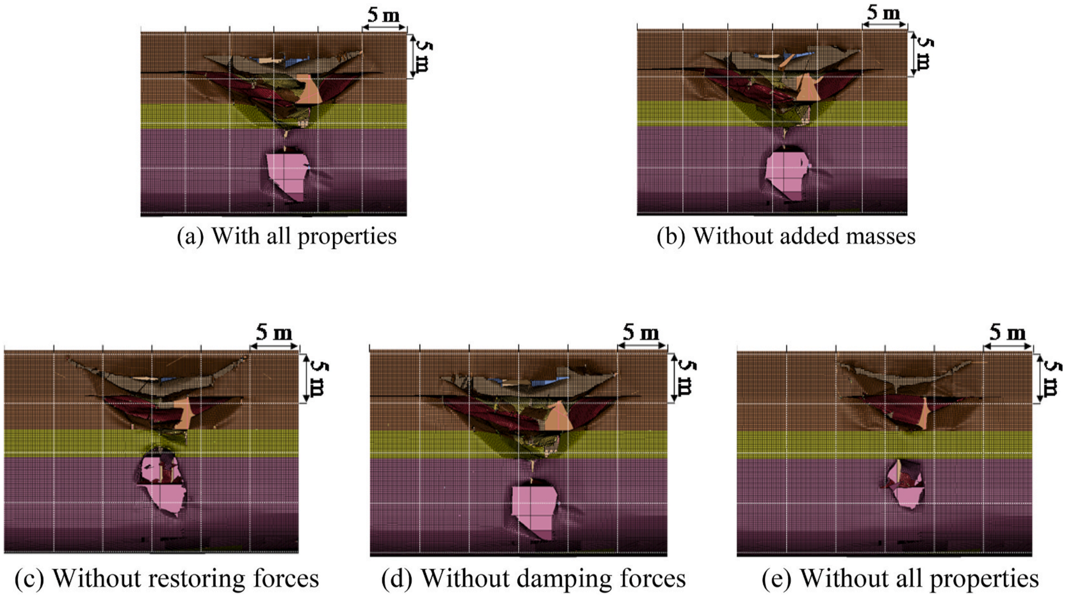

Fig. 15. The influence of hydrodynamic properties on damage extends 12 s after collision.

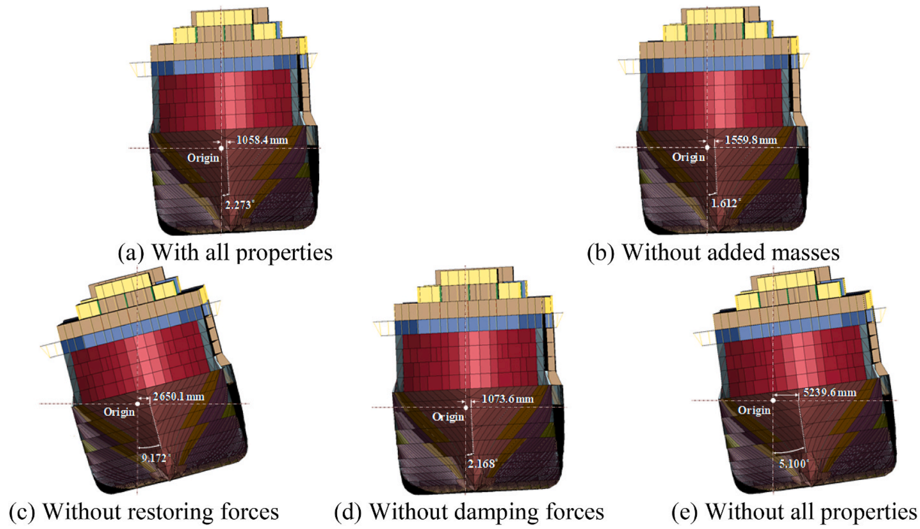

Fig. 16. The influence of hydrodynamic properties on sway and roll motions 12 s after collision.

12=0.09 m/s with added mass vs. 1.560/12=0.13 m/s without added mass) during collision (see Fig. 16(a) and (b)). The restoring force significantly affects the motions of roll for the struck ship and pitch during grounding.

5.3. The influence of hydrodynamic resistance

Fig. 19 shows the results of collision analysis with and without the influence of hydrodynamic resistance force. When the resistance force is accounted for the struck ship only, penetration length increases because of the so-called 'push-back' effect. This same effect is opposite for the case of the striking ship because the kinetic energy is overtaking the potential energy generated during the event. The resistance force on the struck ship is dominant on the penetration and absorbed energy of the struck ship (Fig. 19(a) and (c)). On the other hand, the energy content of the striking ship is mostly affected by the force she receives during the accidental event (Fig. 19(d)). When hydrodynamic resistance forces are applied on both ships, the effect of resistance force is small as hydrodynamic actions and associated ship dynamics balance out (i.e. while we have small damage due to resistance force on striking ship the damage due to resistance force on struck ship is large). Fig. 20 confirms that the effect of hydrodynamic resistance on grounding induced structural dynamic response is minor possibly due to the fact that associated hydrodynamic actions are sharply decreased during the accident

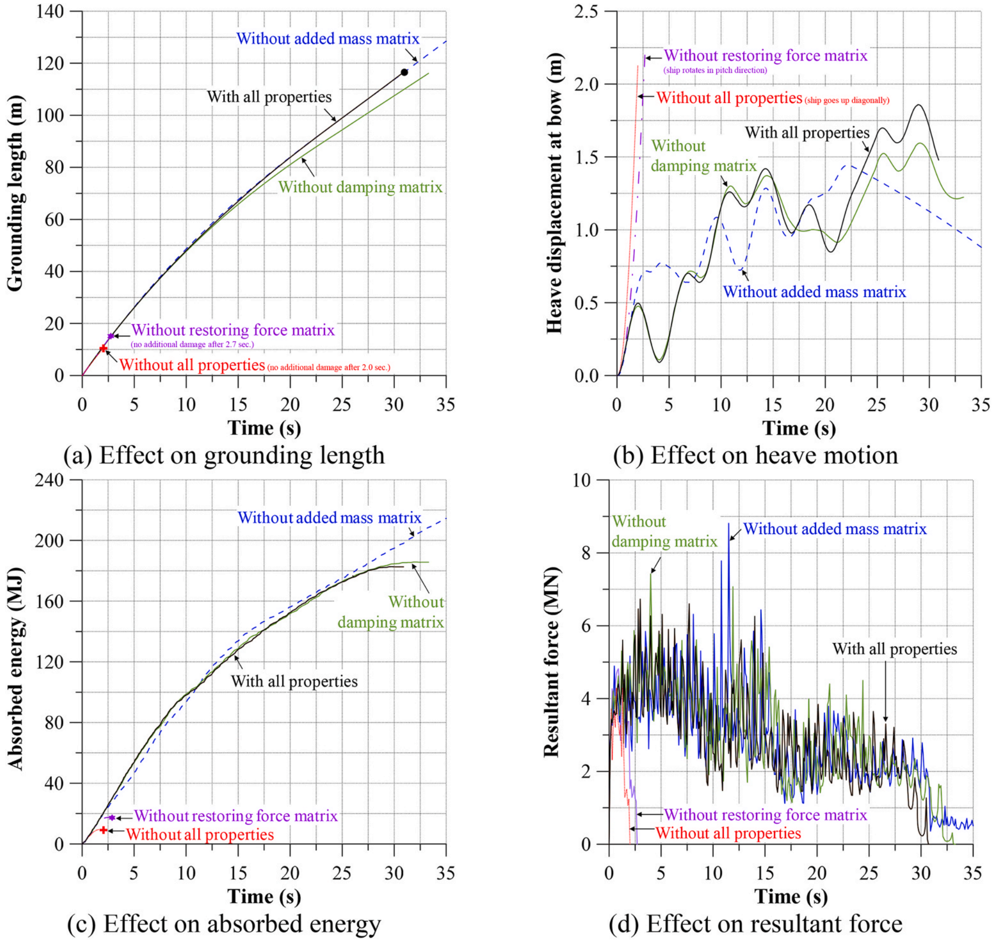

Fig. 17. The influence of hydrodynamic properties in groundings.

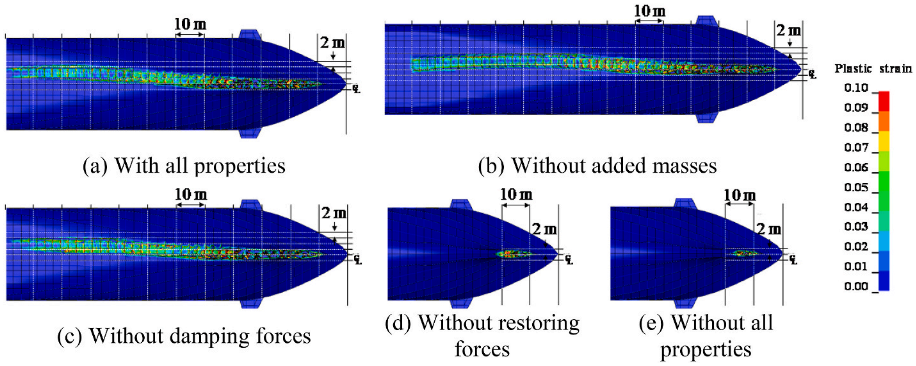

Fig. 18. The influence of hydrodynamic properties on damage extents at the end of grounding event.

(see also Fig. 10 demonstrating resistance force time history).

5.4. Summary

Table 7 confirms that the maximum structural dynamic response following collision or grounding is sensitive to FSI effects. Yet, the level of amplification of results may vary and mostly depends on the influence of hydrodynamic restoring forces during the accident. Fig. 21 compares the structural crashworthiness (penetration or grounding length vs. absorbed energies) regardless of time for collision

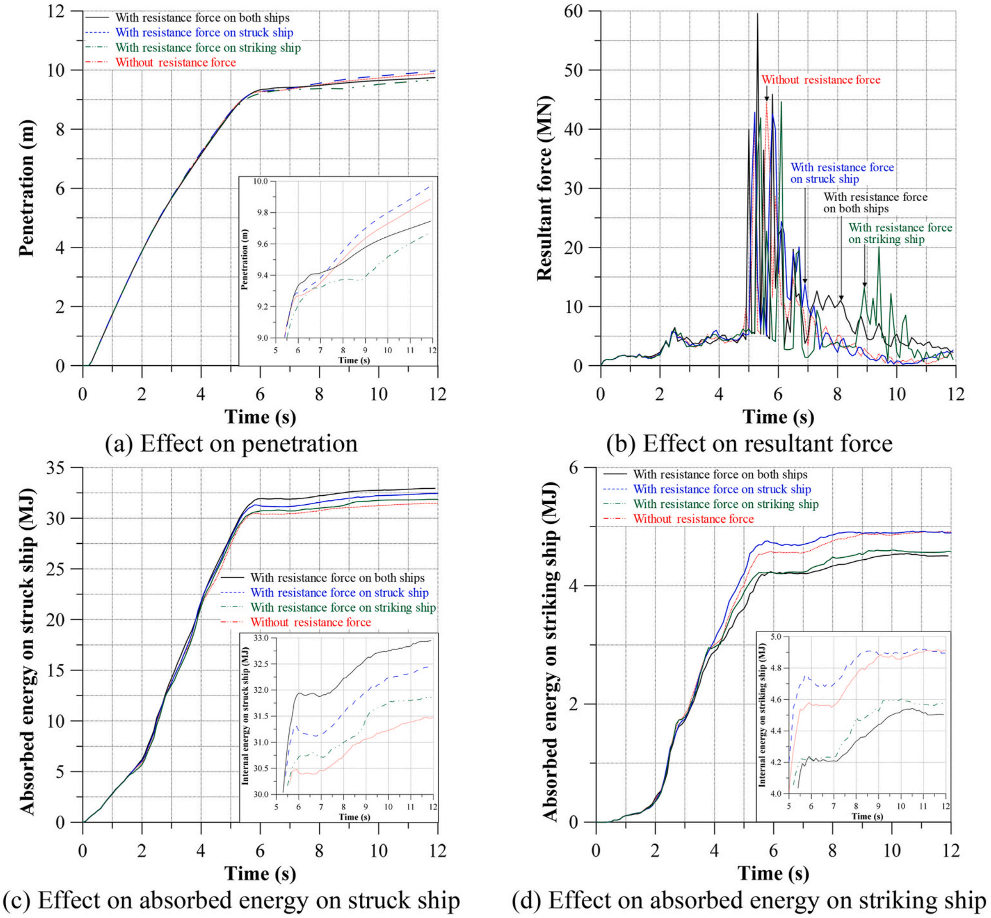

Fig. 19. The influence of resistance force in collisions.

(see Fig. 21(a)) and grounding (see Fig. 21(b)). Fig. 21 shows that the traditional approach (see C-ref and G-ref in Table 7(a) and (b)) that does not consider the effects of FSI associated with maneuvering and hydrodynamic resistance underestimates the structural resistance. On the other hand, the same C-ref and G-ref values (see Table 7(a) and (b)) overestimate the damage (penetration and grounding length) at the same energy level. This observation could be important from a standards development perspective, especially considering that existing rules account only for kinetic energy effects to assess structural capacity or response.

6. Conclusions

This paper explored the influence of multi-physics on the dynamic response of passenger ships subject to collision and grounding accidents. The model introduced accounted for (a) the initial impact velocity in 6-DoF following zig-zag maneuvering analysis as per Taimuri (2020); (b) hydrodynamic properties associated with the influence of surrounding water (restoring force, added mass and damping forces) by potential flow theory, and (c) hydrodynamic resistance forces that reflect that change of velocity during accidents via CFD RANS simulations. The results presented suggest that FSI effects associated with hydrodynamic restoring forces may be the most influential on the structural dynamic response. It was found that the initial velocities of the sway force component of the struck ship and the surge velocity of striking ship may affect the penetration following the collision event. Key conclusions may be summarised as follows:

- Modelling the effects of FSI is useful in terms of understanding the influence of hydrodynamics on dynamic response and eventually the ship's crashworthiness.
- The major influence of restoring forces affect both structural damages and absorbed energy. This is because they restrict roll motion in collision accidents and pitch motion in grounding events.
- Accounting for the effects added mass may lead to smaller damage extents in grounding (see Fig. 17(a)), but bigger damage in collision (see Fig. 14(a)).
- The influence of hydrodynamic damping on ship dynamics relates mostly with the absorbed energy of the system that decreases proportionally with the decreasing amplitude of ship motions.

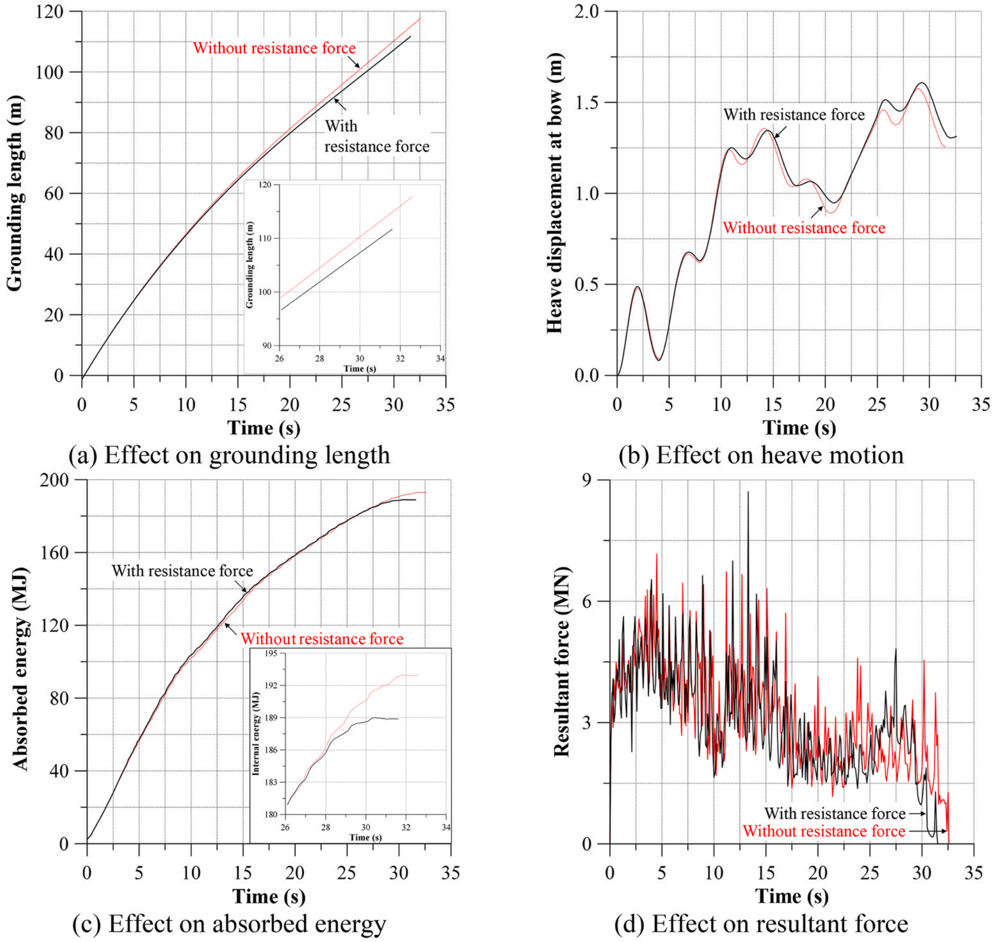

Fig. 20. The influence of resistance force on grounding.

Table 7a
Comparison of structural responses on struck ship at 12 s after collision.

No.	C-ref	C-1	C-2	C-3	C-4	C-5	C-6	C-7	C-8
Related		Velocity	Hydrodynamic properties				Resistance force		
Impact velocity	Surge	6-DoF	Surge	Surge	Surge	Surge	6-DoF		
Added mass	O	O	X	O	O	X	O	O	O
Restoring	O	O	O	X	O	X	O	O	O
Damping	O	O	O	O	X	X	O	O	O
Resistance force	X	X	X	X	X	X	On both	Only struck	Only striking
Penetration (m)	10.43	9.85	10.00	8.97	10.44	6.80	9.75	9.98	9.68
	(0.00)	(-5.56)	(-4.08)	(-14.00)	(0.11)	(-34.81)	(-0.97)*	(1.35)*	(-1.67)*
Absorbed energy on struck ship (MJ)	32.93	30.79	31.52	26.22	33.13	14.22	32.96	32.46	31.86
	(0.00)	(-6.49)	(-4.28)	(-20.36)	(0.62)	(-56.82)	(7.04)*	(5.41)*	(3.46)*

Note: O signifies that the scenario considers the effect, and X means the scenario doesn't take the parameter.
Note: ( ) is the difference in % compared with C-ref, and ( )* is the difference in % compared with C-1.

- The surge velocity of striking or grounded ship is the most important factor affecting the extents of damage during collision or grounding events. The sway velocity of a struck or grounded ship is less critical than surge velocity. This is because the sway speed is much slower than the surge speed (see effects of velocity in 6 DoF in Figs. 12(a) and 13(a)). However, it significantly affects the extent of damage in directions other than the grounding length during collisions/groundings.
- From an overall perspective, the effect of resistance forces seems minor. Yet, for the case of collision, there are indications that hydrodynamic resistance actions could lead to some marginal increase of the structural absorbed energy and hence forces leading to structural deformation.

Table 7b
Comparison of structural responses in grounding at the end of grounding.

No.	G-ref	G-1	G-2	G-3	G-4	G-5	G-6
Related		Velocity	Hydrodynamic properties				Resistance force
Impact velocity	Surge	6-DoF	Surge	Surge	Surge	Surge	6-DoF
Added mass	O	O	X	O	O	X	O
Restoring	O	O	O	X	O	X	O
Damping	O	O	O	O	X	X	O
Resistance force	X	X	X	X	X	X	O
Grounding length (m)	116.50	117.95	128.49	14.95	116.12	10.37	111.70
	(0.00)	(1.24)	(10.29)	(-87.17)	(-0.33)	(-91.10)	(-5.30)*
Absorbed energy (MJ)	182.68	192.96	214.64	17.58	185.76	9.65	188.99
	(0.00)	(5.63)	(17.50)	(-90.38)	(1.69)	(-94.72)	(-2.06)*

Note: O signifies that the scenario considers a parameter, and X means the scenario doesn't take the effect.
Note: ( ) is the difference in % compared with G-ref, and ( )* is the difference in % compared with G-1.

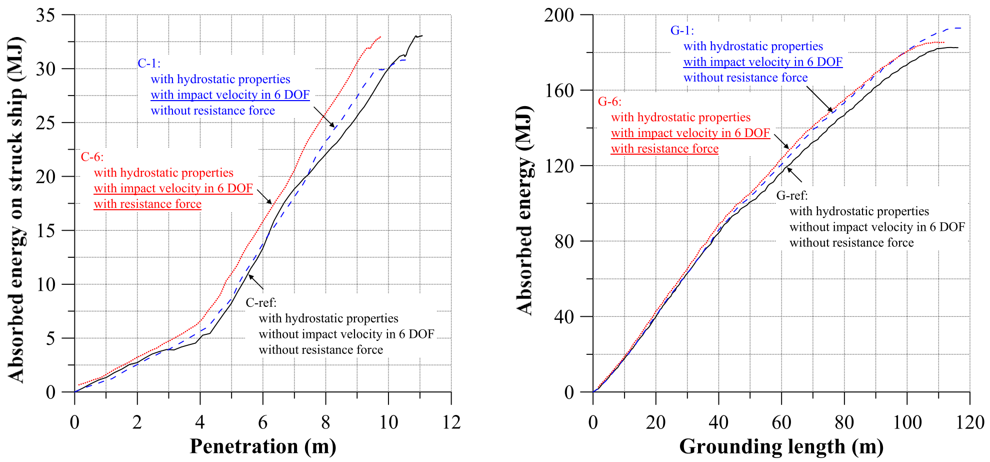

(a) In collision (b) In grounding

Fig. 21. The influence of hydrodynamic simulations on the crashworthiness of ship structures.

Declaration of competing interest

The authors declare that they have no known competing financial interests or personal relationships that could have appeared to influence the work reported in this paper.

Acknowledgement

The research presented in the paper has been carried out under EU Horizon_2020 project FLooding Accident REsponse (FLARE – Contract No. 814753). Special thanks of appreciation are conveyed to (a) Meyer Turku and NAPA for providing the FEA ship models used in this study; (b) CSC Finland for the use of their supercomputing facilities. Mihkel Kõrgesaar and Nima Ahmadi acknowledge the financial support by the Estonian Research Council grant PSG526. Spyros Hirdaris acknowledges financial support from the Academy of Finland University competitive funding award (SA Profi 2-T20404).

References

[1] BV. Hydrostar for experts under manual. Paris, France: Bureau Veritas; 2019.
[2] Chakraverty S, Mahato NR, Karynakar P, Rao TD. Chapter 7 finite volume method in advanced numerical and semi-analytical methods for differential equations. New Jersey, USA: John Wiley & Sons; 2019.
[3] Chapchap A, Hudson DA, Temarel P, Ahmed TM, Hirdaris SE. The influence of forward speed and nonlinearities on the dynamic behaviour of a container ship in regular waves. Trans. Royal Institut. Naval Architect. Part A: Int. J. Mar. Eng. Special Issue Honor William Froude 2011;153(2):137–48. https://www.researchgate.net/publication/259584916_The_influence_of_forward_speed_and_nonlinearities_on_the_dynamic_behaviour_of_a_container_ship_in_regular_waves.
[4] CNN. Oil spill from sunken ferry in Philippines hurts coastline, fishermen. Atlanta, USA: CNN; 2013. https://edition.cnn.com/2013/08/20/world/asia/philippines-ferry-disaster.
[5] CNN. Two Carnival cruise ships collided in Cozumel, Mexico. Atlanta, USA: CNN; 2019. https://edition.cnn.com/2019/12/20/business/carnival-cruise-collision-cozumel-mexico/index.html.
[6] DNV·GL. Evaluation of risk from raking damages due to grounding. Oslo, Norway: DNV·GL; 2015. final report, EMSA/OP/10/2013.

[7] Ehlers S, Tabri K, Romanoff J, Varsta P. Numerical and experimental investigation of the collision resistance of the X-core structure. Ships Offshore Struct 2010;7 (1):21–9. https://www.tandfonline.com/doi/full/10.1080/17445302.2010.532603.
[8] EMSA. Annual overview of marine casualties and incidents 2019. Lisbon, Portugal: European Maritime Safety Agency; 2019.
[9] Ferry M, Le Sourne H, Besnier F. MCOL user's manual, Principia Marine. 2002 [Nantes, France].
[10] Glykas JA, Das KP. Energy conservation during grounding with rigid slopes. Ocean Eng 2001;28(4):397–415. https://www.sciencedirect.com/science/article/pii/S0029801800000020#!.
[11] Haris S, Amdahl J. Crushing resistance of a cruciform and its application to ship collision and grounding. Ships Offshore Struct 2012;7(2):185–95. https://www.tandfonline.com/doi/full/10.1080/17445302.2010.536392.
[12] Hirdaris SE, Lee Y, Mortola G, Incecik A, Turan O, Hong SY, Kim BW, Kim KH, Bennett S, Miao SH, Ternarel P. The influence of nonlinearities on the symmetric hydrodynamic response of a 10,000 TEU container ship. Ocean Eng 2016;111:116–78. https://www.sciencedirect.com/science/article/pii/S002980181500596X.
[13] Holtrop J, Mennen GG. An approximate power prediction method. Int Shipbuild Prog 1982;29(335):166–70. https://content.iospress.com/articles/international-shipbuilding-progress/isp29-335-01.
[14] Hong L, Amdahl J. Plastic mechanism analysis of the resistance of ship longitudinal girders in grounding and collision. Ships Offshore Struct 2008;3(3):159–71. https://www.tandfonline.com/doi/full/10.1080/17445300802263849.
[15] IACS. Common structural rules for bulk carriers and oil tankers. London, UK: International Association of Classification Societies; 2019.
[16] ITOPF. Oil tanker spill statistics 2018. London, UK: The International Tanker Owners Pollution Federation; 2019.
[17] Jones N. Some resent development in the dynamic inelastic behavior of structures. Ships Offshore Struct 2006;1(1):37–44. https://www.tandfonline.com/doi/abs/10.1533/saos.2005.0007.
[18] Jones N. Structural impact. second ed. Cambridge, UK: Cambridge University Press; 2012.
[19] Ko YG, Kim SJ, Sohn JM, Paik JK. A practical method to determine the dynamic fracture strain for the nonlinear finite element analysis of structural crashworthiness in ship-ship collisions. Ships Offshore Struct 2018;13(4):412–22. https://www.tandfonline.com/doi/full/10.1080/17445302.2017.1405584.
[20] Le Sourne H, Couty N, Besnier F, Kammerer C, Legavre H. LS-DYNA application in Shipbuilding. In: Proceedings of 4th European LS-DYNA conference, ulm, Germany; 2003. 23-23 May.
[21] Le Sourne H, Donner R, Besnier F, Ferry M. External dynamics of ship-submarine collision. In: Proceedings of 2nd international conference on collision and grounding of ships, copenhagen, Denmark; 2001. 1-3 July.
[22] Liu B, Villavicencio R, Soares CG. Simplified analytical method to evaluate tanker side panels during minor collision incidents. Int J Impact Eng 2015;78:20–33. https://www.sciencedirect.com/science/article/pii/S0734743X14002899#!.
[23] LSTC. LS-DYNA keyword user's manual. California, USA: Livermore Software Technology Corporation; 2019.
[24] MAIB. Accident report, report No. 4/2020. London, UK: Marine Accident Investigation Branch; 2020.
[25] Matusiak J. Dynamic of a rigid ship. Espoo, Finland: Aalto University Publication Series (SCIENCE+TECHNOLOGY), Aalto University; 2017.
[26] MIT. Marine casualties investigative body: cruise ship Costa Concordia marine casualty on January 13, 2012 report on the safety technical investigation. Roma, Italy: Ministry of Infrastructures and Transports; 2015.
[27] Nguyen TH, Amdahl J, Leira BJ. A study on dynamic grounding of ships. In: Proceedings of the 3rd international conference on marine structures. Hamburg, Germany: March; 2011. p. 28–30.
[28] Paik JK, Kim SJ, Ko YK, Youssef SAM. Collision risk assessment of a VLCC class tanker. In: Proceedings of the society of naval architecture and marine engineers maritime convention 2017, houston, USA; 2017. p. 23–8 [October].
[29] Paik JK, Seo JK. A method for progressive structural crashworthiness analysis under collision and grounding. Thin-Walled Struct 2007;45(1):15–23. https://www.sciencedirect.com/science/article/pii/S0263823107000316.
[30] Pedersen PT, Zhang S. Absorbed energy in ship collisions and groundings revising Minorsky's empirical method. J Ship Res 2000;44(2):140–54. https://orbit.dtu.dk/en/publications/absorbed-energy-in-ship-collisions-and-grounding-revising-minorsk-2.
[31] Pedersen PT, Zhang S. Effect of ship structure and size on grounding and collision damage distributions. Ocean Eng 2000;27(11):1161–79. https://www.sciencedirect.com/science/article/pii/S0029801899000438.
[32] Prabowo AR, Cho HJ, Byeon JH, Bae DM, Sohn JM. Investigation of impact phenomena on the marine structures: part I - on the behavior of thin-walled double bottom tankers during rock-structure interaction. Bali, Indonesia: The 2nd International Joint Conference on Science and Technology; 2017. p. 27–8 [August].
[33] Rudan S, Ćatipović I, Berg R, Völkner S, Prebeg P. Numerical study on the consequences of different ship collision modelling techniques. Ships Offshore Struct 2019;14(S1):387–400. https://www.tandfonline.com/doi/full/10.1080/17445302.2019.1615703.
[34] Samuelides M. Recent advances and future trends in structural crashworthiness of ship structures subjected to impact loads. Ships Offshore Struct 2015;10(5): 488–97. https://www.tandfonline.com/doi/full/10.1080/17445302.2015.1009287.
[35] Sen DT, Vinh TC. Determination of added mass and inertia moment of marine ships moving in 6 degrees of freedom. Int J Transport Eng Technol 2016;2(1): 8–14. http://www.sciencepublishinggroup.com/journal/paperinfo?journalid=514&doi=10.11648/j.ijtet.20160201.12.
[36] Simonsen BC. Ship grounding on rock – II. validation and application. Mar Struct 1997;10(7):563–84. https://www.sciencedirect.com/science/article/pii/S0951833998000033.
[37] SOLAS. Subdivision, watertight and weathertight integrity, SOLAS chapter II-1, Part B-2, international convention for the safety of Life at Sea. London, UK: International Maritime Organization; 2017.
[38] STAR CCM+. User manual for STAR CCM+. Florida, USA: Sabalcore; 2019.
[39] Taimuri G, Mikkola T, Matusiak J, Kujala P, Hirdaris S. The influence of hydrodynamics assumptions on ship maneuvering" Proceedings of 22nd Numerical Towing Tank Symposium. Portugal: Tomar; 2019. p. 29. September - 1 October.
[40] Taimuri G, Mikkola T, Matusiak J, Kujala P, Hirdaris S. A 6-DoF maneuvering model for the rapid estimation of hydrodynamic actions in deep and shallow waters. Ocean Eng 2021. accepted for publication In press.
[41] Wierzbicki T, Abramowicz W. On the crushing mechanics of thin walled structures. J Appl Mech 1983;50(4a):727–34. https://asmedigitalcollection.asme.org/appliedmechanics/article-abstract/50/4a/727/390676.
[42] Youssef SAM, Paik JK. Harzard identification and scenario selection of ship grounding accidents. Ocean Eng 2018;153:242–55. https://www.sciencedirect.com/science/article/pii/S0029801818301185.
[43] Yu Z, Abdahl J. Full six degrees of freedom coupled dynamic simulation of ship collision and grounding accidents. Mar Struct 2016;47:1–22. https://www.sciencedirect.com/science/article/pii/S0951833916300168.
[44] Yu Z, Hu Z, Amdahl J, Liu Y. Investigation on structural performance predictions of double-bottom tankers during shoal grounding accidents. Mar Struct 2013; 33:188–213. https://www.sciencedirect.com/science/article/pii/S0951833913000464.
[45] Zeng J, Hu Z, Chen G. A steady-state plate tearing model for ship grounding over a cone-shaped rock. Ships Offshore Struct 2016;11(3):245–57. https://www.tandfonline.com/doi/full/10.1080/17445302.2014.985429.
[46] Zhang A, Suzuki K. Dynamic FE simulations of the effect of selected parameters on grounding test results of bottom structures. Ships Offshore Struct 2006;1(2): 117–25. https://www.tandfonline.com/doi/abs/10.1533/saos.2006.0117.
[47] Zhang S, Villavicencio R, Zhu L, Pedersen PT. Impact mechanics of ship collisions and validation with experimental results. Mar Struct 2017;52:69–81. https://www.sciencedirect.com/science/article/pii/S0951833916300673?via%3Dihub.
[48] Liu B, Villavicencio R, Zhang S, Soares CG. Assessment of external dynamics and internal mechanics in ship collisions. Ocean Engineering 2017;141:326–36. https://www.sciencedirect.com/science/article/abs/pii/S0029801817303578.